Energy Conversion and Management 52 (2011) 228–235

Contents lists available at ScienceDirect

Energy Conversion and Management

journal homepage: www.elsevier.com/locate/enconman

Proposal and analysis of a high-efficiency combined desalination and refrigeration system based on the LiBr–H_2O absorption cycle—Part 2: Thermal performance analysis and discussions

Yongqing Wang [a,*], Noam Lior [b]

[a] Cleaning Combustion and Energy Utilization Research Center of Fujian Province, Jimei University, Xiamen 361021, PR China
[b] Department of Mechanical Engineering and Applied Mechanics, University of Pennsylvania, Philadelphia, PA 19104-6315, USA

ARTICLE INFO

Article history:
Received 25 January 2010
Accepted 29 June 2010
Available online 27 July 2010

Keywords:
Integrated refrigeration and desalination system
Refrigeration
Water desalination
Combined cycles
Absorption refrigeration/heat pump
Multi-effect evaporation water desalination
Cogeneration

ABSTRACT

This paper continues and concludes the study of the proposed high-efficiency combined desalination and refrigeration system based on the LiBr–H_2O absorption cycle introduced in the paper that is Part 1 [Proposal and analysis of a high-efficiency combined desalination and refrigeration system based on the LiBr–H_2O absorption cycle––Part 1: System configuration and mathematical model. Energy Convers Manage 2010;52:220–7], in which also the mathematical model and its validation are presented in detail. Specifically, the thermal performance of the proposed ARHP–MEE (absorption refrigeration heat pump integrated with a multi-effect evaporation desalter) system, is analyzed, and a parametric sensitivity analysis and a rough economic evaluation are carried out, to clarify and quantify the performance of this combined refrigeration and water system. Typically, driving steam with saturation pressure of 0.15–0.35 MPa and corresponding saturation temperature of 111.4–138.9 °C is applied to run the system. The combined system has good internal synergy, as demonstrated by an energy saving rate of 42% compared with the separate refrigeration-only and water-only systems in a base-case study. The refrigeration-heat cogenerated ARHP subsystem is the main reason for the synergy, with a coefficient of performance of about 1.6 and exergy efficiency above 60% when driven by 0.25 MPa saturated steam. A rough economic analysis indicates qualitatively that there is no penalty in capital equipment for an ARHP–MEE system when compared with the two single-purpose systems, and the higher energy utilization rate of the system makes the energy/operating cost lower.

1. Introduction

The objective of this two-part paper is to propose and study the performance of a proposed heat-driven refrigeration and water cogeneration system combined of a single-effect LiBr–H_2O absorption refrigeration heat pump (ARHP) and a low-temperature multi-effect evaporation (MEE) seawater desalination unit. Following the introduction of the system configuration and the presentation and validation of the mathematical model of the combined system in Part 1 [1], this is Part 2 of the paper, focusing on the thermal performance analysis using this model and some discussions of the system.

The flow chart of the proposed system is shown in Fig. 1. The driving steam (1) heats the LiBr–H_2O mixture in the generator G and boils off the water in it. This steam (9) generated in G is routed into the evaporator, ED_1, of the first effect of MEE, providing the heat for seawater evaporation by releasing its sensible and latent heat. Its condensate (10) is subcooled by the ambient seawater, throttled and then introduced into the ARHP evaporator ER to produce refrigeration. The refrigerant vapor (13) from ER enters the absorber A, and the absorption heat is taken away by the cooling seawater (16).

The ARHP–MEE combined system is composed of two subsystems: ARHP composed of generator G, absorber A, condenser ED_1, evaporator ER, solution heat exchanger SH and subcooler SC, and MEE composed of evaporators (ED_1–ED_n), flashing boxes (F_2–F_n), seawater preheaters (H_1–H_{n-1}) and condenser CD. It is clear that the two subsystems are linked by ED_1, which is both the condenser of the ARHP and the evaporator of the MEE. Producing refrigeration (in ER) and heat (in ED_1) simultaneously, the ARHP subsystem works as both a refrigeration unit and a heat pump.

The performance criteria used in the analysis were discussed in detail in Part 1, with the main ones shown here. Refrigeration–water ratio (RWR):

$$RWR = \frac{Q_R}{m_w}\,[\mathrm{kJ/kg}] \tag{1}$$

* Corresponding author. Tel.: +86 592 6180597; fax: +86 592 6183523.
E-mail address: yongqing@jmu.edu.cn (Y. Wang).

0196-8904/$ - see front matter © 2010 Elsevier Ltd. All rights reserved.
doi:10.1016/j.enconman.2010.06.064

Nomenclature

A	heat-transfer area (m^2)
BPE	boiling point elevation (°C)
COP_{RT}	coefficient of performance of refrigeration-heat cogeneration system
$E_{T,in}$	thermal exergy input to the system (kW)
E_R	exergy of produced refrigeration (kW)
E_T	thermal exergy output for MEE (kW)
m	mass flow rate (kg/s)
m_1	mass flow rate of motive steam (kg/s)
m_W	mass flow rate of produced fresh water (kg/s)
p	pressure (kPa) (MPa)
p_1	motive steam pressure (MPa)
p_{10}	pressure of heating steam for MEE (kPa)
Q	thermal energy; heat load (kW)
Q_{in}	thermal energy input to the system (kW)
Q_R	produced refrigeration (kW)
Q_T	thermal energy output for MEE (kW)
RWR	refrigeration–water ratio (kJ/kg)
T	temperature (°C) (K)
T_{10}	condensation temperature of heating steam in the first effect of MEE (°C)
U	overall heat-transfer coefficient (W/m^2 K)
W_P	pump work (kW)
X	mass concentration of LiBr–H_2O solution (%)
x_v	mass fraction of vapor
ε_R	exergy efficiency of producing E_R (%)
ε_T	exergy efficiency of producing E_T (%)
ε_{RT}	exergy efficiency of refrigeration-heat cogeneration system (%)
ξ	dimensionless exergy destruction (%)
ξ_{others}	dimensionless exergy destruction in ARHP except that in absorber, generator and solution heat exchanger (%)
ΔT_{1-6}	generator approach temperature (°C)

Abbreviations and subscripts

A	absorber
AHP	absorption heat pump
AR	absorption refrigeration
ARHP	absorption refrigeration heat pump
ED	evaporator for desalination
ER	evaporator for refrigeration
G	generator
MEE	multi-effect evaporation
SC	subcooler
SH	solution heat exchanger
V	throttling valve
0	base-case

Coefficient of performance and exergy efficiency of the refrigeration-heat ARHP subsystem:

$$COP_{RT} = \frac{Q_R + Q_T}{Q_{in} + W_{P,ARHP}} \tag{2}$$

$$\varepsilon_{RT} = \varepsilon_R + \varepsilon_T = \frac{E_R}{E_{T,in} + W_{P,ARHP}} + \frac{E_T}{E_{T,in} + W_{P,ARHP}} \tag{3}$$

where Q_T and Q_R are thermal energy and refrigeration, E_R and E_T are thermal exergy and cold exergy, output by ARHP,

$$Q_T = m_9(h_9 - h_{10}) \tag{4}$$

$$Q_R = m_{13}(h_{13} - h_{12}) \tag{5}$$

$$E_T = m_9[h_9 - h_{10} - T_0(s_9 - s_{10})] \tag{6}$$

$$E_R = m_{13}[h_{13} - h_{12} - T_0(s_{13} - s_{12})] \tag{7}$$

Q_{in} and $E_{T,in}$ are thermal energy and thermal exergy input into the ARHP subsystem, which is also the thermal energy and exergy input into the entire ARHP–MEE system,

$$Q_{in} = m_1(h_1 - h_2) \tag{8}$$

$$E_{T,in} = m_1[h_1 - h_2 - T_0(T_1 - T_2)] \tag{9}$$

ε_R and ε_T are the exergy efficiency of producing E_R and E_T, and $W_{P,ARHP}$ is the pumping work consumed in ARHP. Besides, a dimensionless exergy destruction parameter, ξ, is used to evaluate the process irreversibility:

$$\xi = \frac{E_d}{E_{T,in} + W_P} \tag{10}$$

where E_d is exergy destruction, and W_P is the pumping work consumed in the ARHP–MEE system.

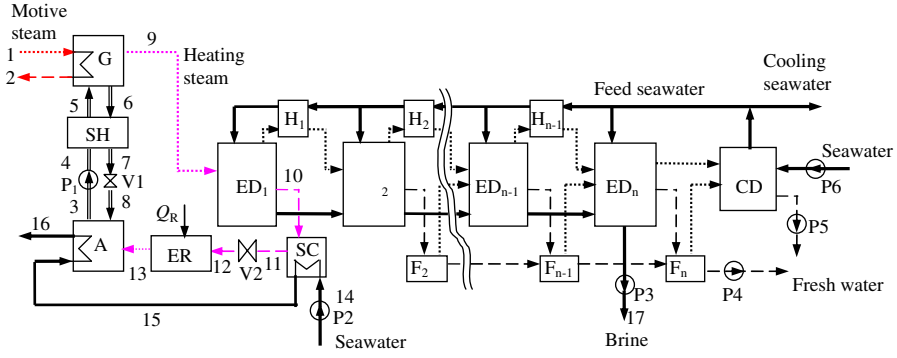

Fig. 1. Schematic diagram of the proposed ARHP–MEE cogeneration system.

2. Base-case performance

The main assumptions for the base-case calculation of the cogeneration system are summarized in Table 1. After referring to the operating conditions of an existing MEE unit [2], a six-effect MEE was chosen and the performance simulated. The main parameters of the base-case of ARHP–MEE are shown in Table 2.

To clarify the synergy of the proposed combined system, comparison is performed between the ARHP–MEE combined system and two separate single-product systems: a typical refrigeration-only single-effect LiBr–H_2O absorption refrigeration (AR) system which has the same configuration and working process with the ARHP subsystem except that ED_1 is replaced by an condenser and the condensation heat is released to the ambient, and a water-only absorption heat pump (AHP) driven MEE system which is much similar to ARHP–MEE except that the subcooler SC, the throttling valve V_2 and the refrigeration evaporator ER are eliminated, the vapor absorbed in the absorber is from the last effect of MEE and the absorption heat is also used to produce heating steam for MEE. The base-case parameters of AR and AHP–MEE are shown in Table 3, and the comparison results are shown in Table 4.

The energy saving of the combined system (compared with the single-product systems) is significant, about 42% for the base-case. It is the ARHP subsystem that contributes to this substantial improvement. Tables 5 and 6 show the energy and exergy use of the ARHP. For the ARHP, the output cold and thermal energy account for 75.6% and 77.9% of the input energy, respectively, resulting in a total coefficient of performance, COP_{RT}, of 1.54, which is considerably higher than the COP of 0.77 of the refrigeration-only unit running under the same conditions. The refrigeration exergy and the thermal exergy produced are 26.6% and 33.7%, respectively, of the total input exergy, leading to a total exergy efficiency of 60.3%, much higher than the 27% of exergy efficiency of the refrigeration-only unit. So, raising the condensation temperature, T_{10}, of the generator-produced vapor at 65 °C in this case (higher than the 40 °C in a conventional refrigeration-only unit), a temperature high enough to make the condensation heat suitable for driving the desalination MEE, leads to an additional gain of 33.7% of thermal exergy or 77.9% of thermal energy, at the cost of only 0.4% decrease of produced cold exergy or 1.4% decrease of cold energy. Typically the refrigeration capacity of real AR units decreases distinctly with the increase of the condensation temperature T_{10} (for instance, one example [3] shows that for 1 °C of increase in T_{10}, Q_R decreases by 5–7%), primarily because the motive steam mass flow m_1 and the strong-and-weak-solution concentration difference ΔX both decrease with increasing T_{10}, with further explanation in [3]. Different from real units, m_1 and ΔX are kept constant at the base-case analysis.

Table 1
Main assumptions for the base-case calculation.

Ambient conditions	
Temperature	30 °C
Pressure	1 atm
Salinity of seawater	35,000 ppm
Generator	
Mass flow rate of motive steam, m_1	1 kg/s
Motive steam pressure p_1 (saturation temperature T_1)	0.25 MPa (127.4 °C)
Generator approach temperature in AHP and ARHP subsystems, $\Delta T_{1\text{-}6}$	10 °C
Mass concentration difference between strong-and-weak-solutions, ΔX	5%
Absorber	
Absorber approach temperature	5 °C
Absorbed vapor pressure minus absorber operation pressure	40 Pa
Solution heat exchanger	
Temperature difference at the cold side	10 °C
Minimum temperature difference between outlet strong solution and crystallization point	15 °C
Evaporator for refrigeration	
Refrigerant evaporation temperature (pressure)	6 °C (0.935 kPa)
Condenser for AR unit	
Condensation temperature (pressure)	40 °C (7.38 kPa)
Subcooler	
Subcooler approach temperature	5 °C
MEE unit	
Number of effects	6
Salinity of the discharge brine	70,000 ppm
Temperature rise of seawater in preheater	4 °C
Condensation temperature T_{10} (pressure p_{10}) of heating steam in the 1st effect	65 °C (25.02 kPa)
Temperature difference at the hot side of end condenser CD	4 °C
Operation temperature in the last effect	43 °C

3. Sensitivity analysis and parameter range

Under the specified ambient conditions, the main factors influencing the performance of the ARHP–MEE system are: generator approach temperature $\Delta T_{1\text{-}6}$, LiBr–H_2O strong-and-weak solution concentration difference ΔX, motive steam pressure p_1, and the heating-steam condensation temperature T_{10} in the first desalination evaporator ED_1 (or the generator operation pressure). The performance of the MEE unit certainly has great influence on the whole system, with the discussions not included in this paper. Detailed information on MEE unit can be found in many publications (cf. [4,5]).

3.1. Sensitivity to the generator approach temperature $\Delta T_{1\text{-}6}$

Fig. 2 shows the mass flow of produced water, m_W, produced refrigeration, Q_R, and the exergy of the produced refrigeration, E_R, of the ARHP–MEE system for different $\Delta T_{1\text{-}6}$ and p_1, with the other conditions kept constant at the base-case values shown in Table 1. To exhibit more clearly the sensitivity of water and refrigeration production in the combined system, the values of m_W, Q_R and E_R are normalized by their base-case values shown in Tables 2 and 6.

Fig. 2 reveals that different input conditions generate different ranges of $\Delta T_{1\text{-}6}$. For instance, the range of $\Delta T_{1\text{-}6}$ is 9–13 °C when p_1 = 0.25 MPa and T_{10} = 65 °C, and 20–24.5 °C when p_1 is changed to 0.35 MPa. The increase of $\Delta T_{1\text{-}6}$ causes the operation temperature of the generator and then that of the absorber to decrease. The temperature of the cooling medium used in the absorber determines the lowest absorber outlet temperature, and then the upper limit of $\Delta T_{1\text{-}6}$. The low limit of $\Delta T_{1\text{-}6}$ is determined by two factors: one is the minimal $\Delta T_{1\text{-}6}$ technically allowed, which is taken as 5 °C in this paper, and the other is the strong-solution crystallization temperature, which rises with the decrease of $\Delta T_{1\text{-}6}$ (for specified p_1 and T_{10} and then specified T_1 and p_{10}, a lower $\Delta T_{1\text{-}6}$ causes a higher T_6 and then a higher X_6 for remaining a constant p_{10}, resulting in a higher crystallization temperature of the strong solution), thus making the solution easier to crystallize and restricting the reduction of $\Delta T_{1\text{-}6}$. The low limit of $\Delta T_{1\text{-}6}$ is the higher of the $\Delta T_{1\text{-}6}$ values determined by these two limits, one determined by the minimal values needed for practical heat-transfer and the other the crystallization temperature.

The m_W and Q_R (E_R) of ARHP–MEE increase with $\Delta T_{1\text{-}6}$ (Fig. 2), and reach the highest value under the upper limit of $\Delta T_{1\text{-}6}$. Our calculations show that, for 1 °C of increase in $\Delta T_{1\text{-}6}$, both refrigeration

Table 2
The main parameters of the base-case of the ARHP–MEE system.

		T (°C)	p (kPa)	m (kg/s)	X (% LiBr)	x_v
ARHP subsystem						
Motive steam		*127.4*	*250*	*1*	0	1
Strong solution from generator G		117.4	*25.02*	7.93	61.72	0
Strong solution from solution heat exchanger SH		47.4	24.77	7.93	61.72	0
Weak solution from absorber A		37.4	0.895	8.62	56.72	0
Weak solution from solution heat exchanger SH		97.8	–	8.62	56.72	0
Steam produced in generator G		111.5	*25.02*	0.7	0	1
Refrigerant before throttling valve V_2		35	–	0.7	0	0
Refrigerant entering evaporator ER		*6*	*0.935*	0.7	0	0.049
Effect number	1	2	3	4	5	6
MEE subsystem						
Feed seawater						
T (°C)	57.9	53.9	49.9	45.9	41.9	37.9
m (kg/s)	1.43	1.39	1.36	1.32	1.29	1.25
Brine						
T (°C)	62.2	58.4	54.5	50.6	46.8	*43*
m (kg/s)	0.71	1.41	2.09	2.75	3.39	4.02
BPE (°C)	0.86	0.84	0.83	0.81	0.8	0.78
Produced vapor						
T (°C)	62.2	58.4	54.5	50.6	46.8	43
p (kPa)	21.2	17.7	14.7	12.2	10.1	8.3
m (kg/s)	0.71	0.7	0.68	0.66	0.64	0.62
Condensate						
T (°C)	*65*	61.0	57.2	53.3	49.5	45.7
m (kg/s)	0.7	0.71	0.7	0.69	0.67	0.66
System production						
Produced refrigeration, Q_R	1652 kW					
Produced fresh water, m_W	4.016 kg/s					
Refrigeration–water ratio, *RWR*	411.4 kJ/kg					

Values in italics are directly from Table 1.

Table 3
The main parameters of the base-case of the AR and AHP–MEE systems.

		T (°C)	p (kPa)	m (kg/s)	X (% LiBr)	x_v
AR system						
Motive steam		*127.4*	*250*	*1*	0	1
Strong solution from generator G		88.0	*7.38*	8.06	61.72	0
Strong solution from solution heat exchanger SH		47.4	7.31	8.06	61.72	0
Weak solution from absorber A		37.4	0.895	8.77	56.72	0
Weak solution from solution heat exchanger SH		72.4	–	8.77	56.72	0
Steam produced in generator G		82.5	*7.38*	0.71	0	1
Refrigerant before throttling valve V		35	–	0.71	0	0
Refrigerant entering evaporator ER		*6*	*0.935*	0.71	0	0.049
Produced refrigeration of AR, Q_R		1681 kW				
AHP subsystem in AHP–MEE system						
Motive steam		*127.4*	*250*	*1*	0	1
Strong solution from generator G		117.4	*25.02*	8.32	61.72	0
Strong solution from solution heat exchanger SH		89.2	24.77	8.32	61.72	0
Weak solution from absorber A		79.2	8.22	9.05	56.72	0
Weak solution from solution heat exchanger SH		103.5	–	9.05	56.72	0
Steam produced in generator G		111.5	*25.02*	0.73	0	1
Steam from absorber A		74.2	*25.02*	0.88	0	0
MEE subsystem in AHP–MEE system						
Effect number	1	2	3	4	5	6
Mass flow of Feed seawater (kg/s)	3.25	3.18	3.11	3.03	2.96	2.89
Mass flow of brine (kg/s)	1.63	3.21	4.76	6.28	7.76	9.20
Mass flow of produced vapor (kg/s)	1.62	1.59	1.55	1.52	1.48	1.44
Mass flow of condensate (kg/s)	1.62	1.63	1.60	1.58	1.55	1.53
Produced fresh water of AHP–MEE, m_W		9.204 kg/s				

Values in italics are directly from Table 1. For MEE subsystem in the AHP–MEE system, only the mass flows of the working fluids are shown in the table, with the other parameters almost the same as that in Table 2.

and water production increase by about 0.3%. Fig. 2 also reveals that refrigeration and water production have the same trend with the variation of ΔT_{1-6}, and that the refrigeration–water ratio *RWR* remains almost constant. The reason is that it is the same stream of working fluid, i.e. the vapor produced in the generator, that produces both the desalination heat (in evaporator ED_1) and the refrig-

Table 4
Comparison between the combined system and the separate refrigeration and water systems.

	ARHP–MEE combined system	AHP–MEE water-only system	Absorption refrigeration system
Operation pressure of generator, kPa	*25.02*	*25.02*	*7.38*
Operation pressure of absorber, kPa	0.895	8.22	0.895
Condensation temperature of generator-produced steam, °C	*65*	*65*	*40*
Temperature of absorber outlet weak solution, °C	37.4	79.2	37.4
Mass concentration of weak solution, % LiBr	56.72	56.72	56.72
Mass concentration of strong solution, % LiBr	61.72	61.72	61.72
Cooling capacity, kW	1652	0	1652
Produced fresh water, kg/s	4.016	4.016	0
Mass flow of motive steam, kg/s	*1*	0.436	0.983
Total mass flow of motive steam, kg/s	1		1.42

Values in italics are directly from Table 1.

Table 5
Energy utilization of the ARHP subsystem for the base-case.

Components	Heat load (kW)
Generator G	2181
Absorber A	2045
Condenser ED_1	1701
Evaporator ER	1652
Solution heat exchanger SH	1056
Subcooler SC	87.7

	Unit (kW)	Percentage
Thermal energy and pump work input to ARHP	2184	100
Cold energy produced, Q_R	1652	75.6
Thermal energy output for MEE, Q_T	1701	77.9
COP_{RT}	1.54	

Table 6
Exergy utilization of the ARHP subsystem for the base-case.

Components or streams	Exergy destruction (kW)	Dimensionless exergy destruction (%)
Generator G	56	10.5
Absorber A	86.4	16.2
Solution heat exchanger SH	41.4	7.8
Subcooler SC	5.3	1.0
Cooling seawater	15.2	2.8
Others	7.5	1.4

	Unit (kW)	Percentage
Thermal exergy and pump work input to ARHP	533.5	100
Exergy of produced refrigeration, E_R	142.1	26.6
Thermal exergy output for MEE, E_T	179.6	33.7
Exergy efficiency, ε_{RT}	60.3%	

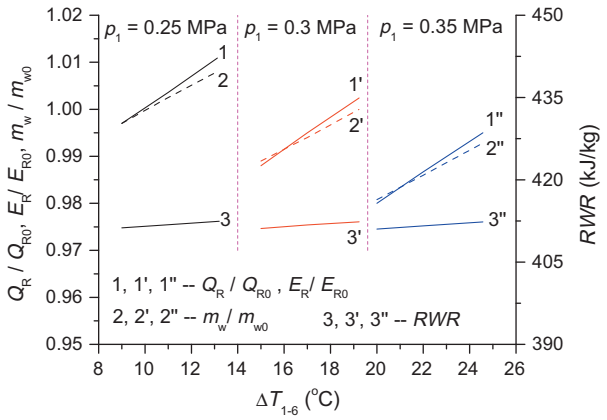

Fig. 2. Effect of the generator approach temperature ΔT_{1-6}.

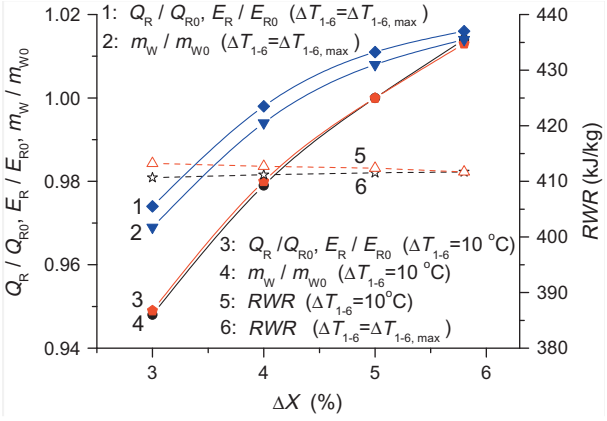

Fig. 3. Effect of the strong-and-weak solution concentration difference ΔX.

eration (in evaporator ER), so when the mass flow of the vapor, m_9, increases with ΔT_{1-6}, both Q_R (or E_R) and Q_T (or E_T) increase at almost the same rate with m_9, resulting in an almost constant *RWR*.

3.2. Sensitivity to the LiBr–H_2O strong-and-weak solution concentration difference ΔX

Fig. 3 shows the influence of the concentration difference, ΔX, between the strong and the weak LiBr–H_2O solutions. The lines 3–5 are for $\Delta T_{1-6} = 10$ °C, and lines 1, 2 and 6 for the maximum ΔT_{1-6} allowed as discussed above. It is revealed that increasing ΔX leads to distinct improvements of water and refrigeration production. When ΔX is increased from 3% to 5.8%, the two outputs both increase by over 6% for $\Delta T_{1-6} = 10$ °C. The reason is the same as in a conventional absorption refrigeration system [3]. Fig. 3 also shows that *RWR* depends only slightly on ΔX, and has almost the same value as that shown in Fig. 2, for the same reasons given in Section 3.1.

The increase of ΔX is limited by the point at which the temperature difference between the strong solution at the solution heat exchanger (SH) outlet and the crystallization point is at the minimum value allowed, 15 °C in this paper as shown in Table 1. Different calculation conditions cause different maximum ΔX. It is around 5.8% within the common parameters range of ARHP–MEE, as shown in Fig. 4 which illustrates the ranges of ΔX and ΔT_{1-6} for different T_{10} and p_1. Higher ΔX leads to higher water and refrigeration production (Fig. 3), but narrower range of ΔT_{1-6} (Fig. 4).

Generally, to get a good thermal performance and at the same time ensure a certain flexibility in operation and design, 4–5% is a suitable range of ΔX for ARHP–MEE system.

3.3. Sensitivity to the condensation temperature T_{10} of the heating steam in ED_1

Since ED_1 is both the condenser of ARHP and the evaporator of MEE, i.e. the interface between the refrigeration and water production subsystems, the condensation temperature, T_{10}, of the heating steam in ED_1 has a great influence on the performance of each of these two subsystems and thus on the performance of the ARHP–MEE combined system.

Fig. 5 shows the refrigeration and heat production, and Fig. 6 shows the exergy utilization, of the ARHP unit, for different T_{10}. With the increase of T_{10}, the outputs Q_R and E_R as well as Q_T drop slightly, while the thermal exergy E_T for MEE rises significantly. The strong increase of E_T is mainly contributed to the decreased exergy destruction in the generator (Fig. 6) where the heat-transfer temperature difference has a distinct decrease with increasing T_{10} (Fig. 7).

Higher T_{10} broadens the operation temperature range of the MEE unit, implying the possibility of running an MEE with more effects than the six chosen for this study. More effects lead to a much higher performance ratio [4]. It is thus clear that for the specified motive heat source, raising T_{10} would cause a minor decrease of refrigeration production but a great potential for producing more fresh water. For instance, increasing T_{10} from 65 °C to 68.4 °C would decrease the cooling capacity by 0.2%, but increase the water production by 15% when the number of effects of the MEE is changed from 6 to 7, without almost any change of the specific heat-transfer area (per kg/s produced fresh water) of the MEE for the two situations.

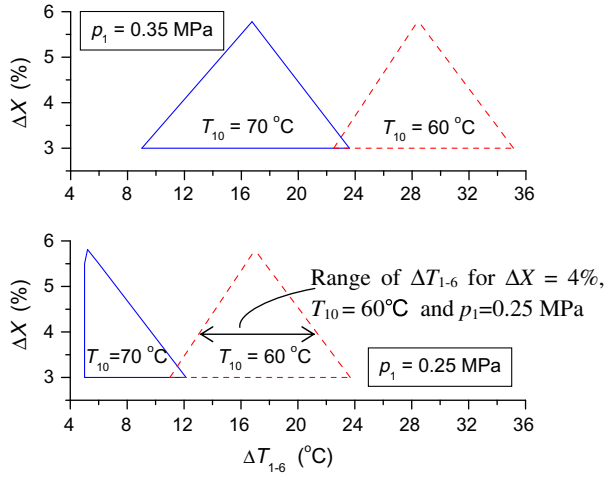

Fig. 4. Ranges of ΔX and ΔT_{1-6} for different T_{10} and p_1.

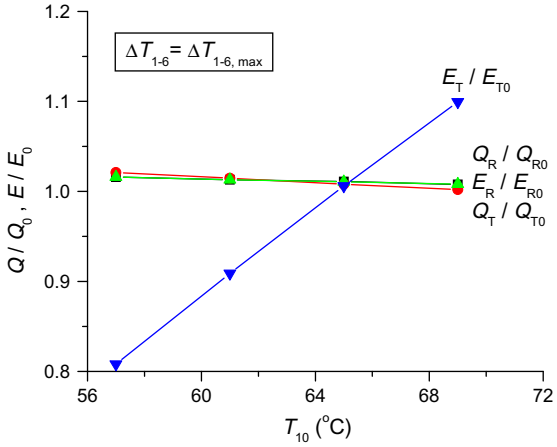

Fig. 5. Effect of the condensation temperature of the MEE heating steam, T_{10}.

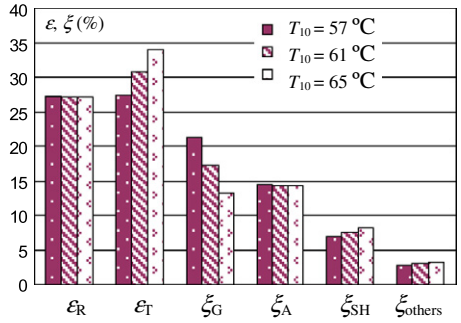

Fig. 6. Exergy utilization of ARHP subsystem for different T_{10}.

3.4. Sensitivity to the motive steam pressure p_1

The motive steam is assumed to be saturated, and Fig. 8 shows the influence of its pressure p_1. Increasing p_1 was found to reduce both water and refrigeration production. This trend can also be seen in Fig. 2. From the properties of saturated steam, based on 1 kg/s motive steam, the thermal energy input to the ARHP–MEE system decreases when p_1 is increased because of the decreased condensation latent heat of the motive steam, while the input thermal exergy increases, with the increase of p_1. The exergy destruction in the generator has a significant rise with p_1 (Fig. 8) because of the consequent enlarged heat-transfer difference in the generator (Fig. 9), resulting in decreased E_R and E_T, and a decreased E_T leads to a decreased m_W (Fig. 8).

The above discussions on the effects of p_1 are performed based on a constant T_{10}. A higher p_1 can allow the raising of the heating steam (stream 9 in Fig. 1) pressure and correspondingly a higher T_{10}. This, in turn, can allow a higher m_W by adding effects to the MEE as discussed in Section 3.3. For instance, with the maximum ΔT_{1-6} allowed and the other conditions kept constant at the base-case values (Table 1), saturated motive steam of 0.15 MPa can produce heating steam with T_{10} = 58 °C at the highest, which

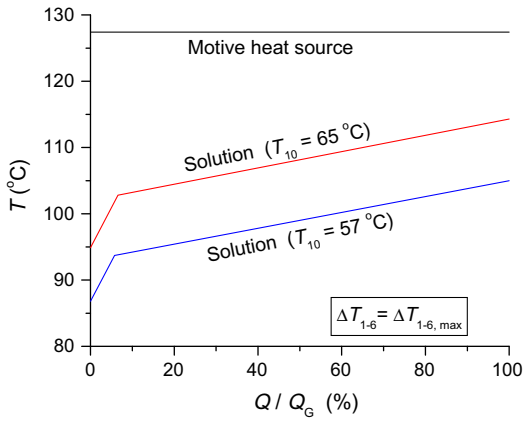

Fig. 7. The generator T–Q diagram for different T_{10}.

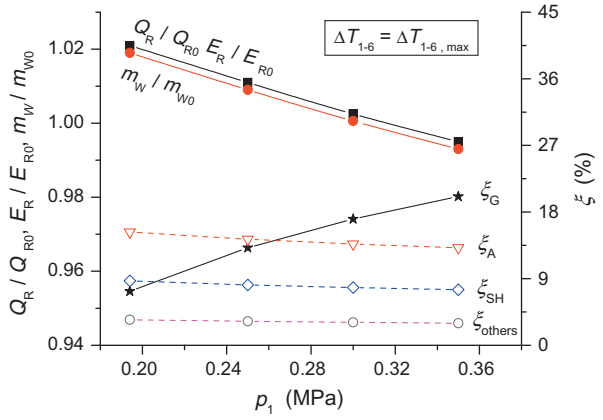

Fig. 8. Effect of the motive steam pressures p_1 under constant T_{10}.

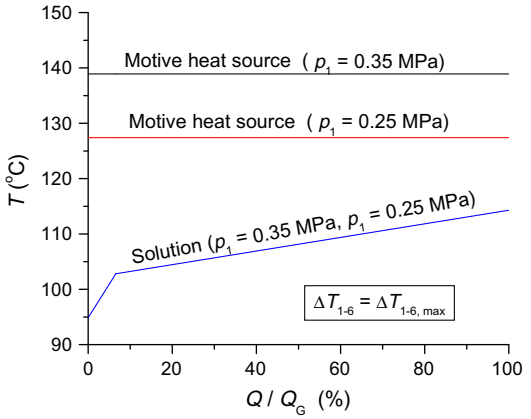

Fig. 9. The generator T–Q diagram for different motive steam pressures p_1 under constant T_{10}.

is suitable to run a four-effect MEE unit, while motive steam of 0.25 MPa has the ability to produce heating steam with T_{10} = 72 °C, suitable to run a seven-effect MEE unit.

Generally, for the typical range of T_{10} from 58 °C to 72 °C, the ARHP–MEE system proposed in this study, which is based on a single-effect absorption refrigeration/heat pump, is applicable to be run by motive steam with p_1 from 0.15 MPa to 0.35 MPa (saturation temperature T_1 from 111.4 °C to 138.9 °C). Further study is needed to find more favorable ways of using higher pressure steam.

4. Discussion

This study is a proposal and analysis of an efficient way of producing both fresh water and refrigeration simultaneously. Being driven mainly by low-grade heat, the proposed system is suitable to be combined with the processes that can provide that type of heat, such as power generation, chemicals production, solar thermal energy, and geothermal energy, to improve the total energy efficiency.

From the discussions in Section 3, we can draw a conclusion that, for a specified ARHP–MEE plant, water and refrigeration production can be regulated in a wide range by changing the operating parameters, but the ratio between the two, *RWR*, remains almost constant. This impossibility to regulate *RWR*, indicates that such an ARHP–MEE plant will be suitable only for conditions where the requirement for refrigeration and fresh water are relatively constant or changes while maintaining the same *RWR*.

The system shown in Fig. 10, which is the integration of an ARHP–MEE and an AHP–MEE, however, can allow changes in *RWR*. By regulating the mass flow of the refrigerant entering ER, the values of m_W, Q_R and *RWR* can be varied in a very wide range. For instance, under the base-case calculation conditions (Table 1), when the vapor produced in the generator is condensed, throttled and then all routed into ER, the system works as a ARHP–MEE system, and 4.016 kg/s of fresh water and 1652 kW of refrigeration can be obtained, with *RWR* = 411 kJ/kg, and when the water mass flow entering ER is zero, the system works as a water-only AHP–MEE system, and 9.204 kg/s of fresh water can be produced with *RWR* having the value of zero. Theoretically, *RWR* can be changed from 0 to 411 kJ/kg, indicating greater flexibility for design and operation.

While a detailed economic analysis was not performed, some basic important observations can be made. The ARHP–MEE system has much fewer components than those needed for the sum of the separate single-purpose systems. For instance, the ARHP subsystem works as a refrigeration unit and a heat pump, and all the components, including the generator, absorber, solution heat exchanger, evaporator, condenser, pumps and valves, are common parts for both refrigeration and heat production and thus do not need to be duplicated as in the separate systems. Obviously, it is not just the number of the components but also their size that determines the capital cost of the ARHP, indicating the necessity for a detailed study.

Since the ARHP–MEE system is composed mainly of heat exchangers, the calculation of heat-transfer area is especially important in economic analysis. To determine the heat-transfer area, the specific type of each heat exchanger must be known, and the heat-transfer coefficient which is also a function of the working fluids properties and flow processes, must be calculated. We here made a very rough comparison between the heat exchanger area needed for the ARHP–MEE combined system and for that of the separate AR refrigeration-only and AHP–MEE water-only systems producing the same amount of refrigeration and water. The comparison is based on the assumption that the heat exchangers are similar with those used in conventional refrigeration and heat pump systems [3], and uses the average typical overall heat-transfer coefficient values for these heat exchanger processes and fluids as found in the literature [3]. Table 7 shows the evaluation results under base-case calculation conditions, where the subcooler SC is not considered because its heat load is very low

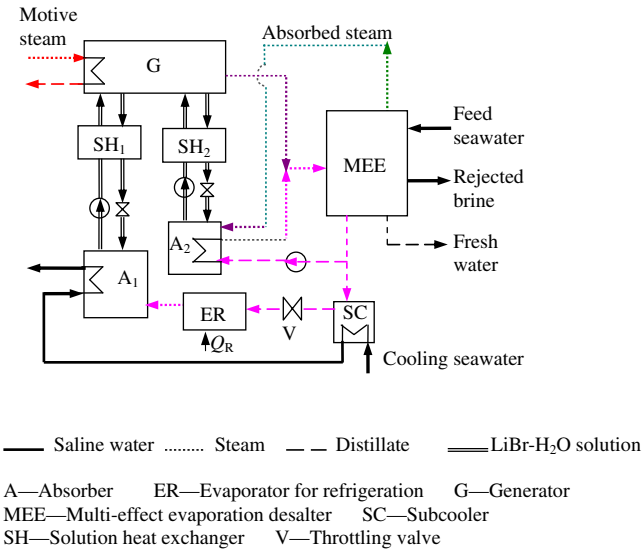

Fig. 10. The integration system of ARHP–MEE and AHP–MEE.

Table 7
A rough comparison of heat-transfer areas of ARHP–MEE with separate systems producing the same outputs.

	Q (kW)	UA (kW/K)	U [2] (W/m^{2}K)	A (m^2)	ΣA (m^2)
ARHP–MEE system					509
Generator	2181	143.7	1160	124	
Absorber	2045	308	1200	257	
Solution heat exchanger	1056	74	580	128	
AR system					432
Generator	2143	47.9	1160	41	
Absorber	2044	283.2	1200	236	
Condenser	1737	340.7	4700	72	
Solution heat exchanger	604	47.9	580	83	
AHP–MEE system					130
Generator	952	62.7	1160	54	
Absorber	910	55.8	1200	47	
Solution heat exchanger	198	16.7	580	29	
AR system and AHP–MEE system					563

compared with the other heat exchangers (Table 5), and the MEEs used in AHP–MEE and ARHP–MEE are also not included because they have the same heat-transfer area for producing the same water outputs and will not influence the comparison result.

Table 7 reveals that the heat-transfer area of the ARHP–MEE system is lower than that of the separate AR and AHP–MEE systems having the same outputs. Different type of heat exchangers and different values of heat-transfer coefficients may lead to greatly different heat-transfer areas from those in Table 7. Although the estimations here are very rough, it demonstrates qualitatively that there is no penalty in capital equipment for an ARHP–MEE system. Another economic advantage is that the higher energy utilization rate of the ARHP–MEE system makes the energy/operating cost lower.

5. Conclusions

Good internal synergy, demonstrated by energy saving, is accomplished by combining an absorption refrigeration/heat pump with low-temperature thermal desalination. In a case study of the ARHP–MEE system, the energy saving rate is 42%, compared with the individual refrigeration-only and water-only systems. Driven by 0.25 MPa saturated steam, the coefficient of performance of the ARHP is around 1.6 and the exergy efficiency above 60%.

A parametric sensitivity analysis of the ARHP–MEE system shows that a higher generator approach temperature and a higher concentration difference between the strong and the weak solution raise water and refrigeration production simultaneously, and using driving steam of higher pressure allows increasing the number of effects of the MEE unit and thus produces more water. The maximum operational strong-and-weak solution concentration difference is around 5.8%, and within a range of 4–5% good thermal performance as well as certain flexibility for design and operation can be achieved. For the typical range of heating-steam condensation temperature from 58 °C to 72 °C, the system is applicable to be run by motive steam with pressure from 0.15 MPa to 0.35 MPa and correspondingly saturation temperature from 111.4 °C to 138.9 °C.

A rough economic analysis indicates qualitatively that there is no penalty in capital equipment for an ARHP–MEE system when compared with the two single-purpose systems, and the higher energy utilization rate of the system makes the energy/operating cost lower.

The outputs of ARHP–MEE can be varied in a wide range but not independently because their ratio remains almost constant. A system combined by ARHP–MEE and AHP–MEE was introduced to meet the requirement of the situations where wider refrigeration–water ratio is needed.

Acknowledgements

The authors gratefully acknowledge the support of the National Natural Science Foundation of China (Project No. 50676023), the Science and Technology Innovation Platform Foundation of Fujian Province, China (Project No. 2009H2006) and the Foundation for Innovative Research Team of Jimei University, China (Project No. 2009A002).

References

[1] Wang Y, Lior N. Proposal and analysis of a high-efficiency combined desalination and refrigeration system based on the LiBr–H_2O absorption cycle––Part 1: system configuration and mathematical model. Energy Convers Manage 2010;52:220–7.
[2] Darwish MA, Alsairafi A. Technical comparison between TVC/MEB and MSF. Desalination 2004;170:223–9.
[3] Dai Y. Technology and application of lithium bromide absorption refrigeration. Beijing: Mechanical Industry; 2002 [in Chinese].
[4] El-Dessouky H, Ettouney H. Fundamentals of salt water desalination. Amsterdam: Elsevier; 2002.
[5] Alasfour FN, Darwish MA, Bin Amer AO. Thermal analysis of ME-TVC+MEE desalination systems. Desalination 2005;174:39–61.